Helosphere

ME 4041

Dr. Yan Wang

Georgia Institute of Technology

North Ave NW, Atlanta, GA 30332

The Team

Michael Fletcher | mike.fletch@gatech.edu

Gunner Robinson | gunnerrobinson@gatech.edu

Jake Tillery | jtillery7@gatech.edu

Table of Contents

Introduction

The Helosphere is a miniature quadcopter specially designed to increase human interaction and handling with drones. It is entirely enclosed by a plastic mesh cage so that the user can catch, throw, and hold the drone without worrying about grasping the drone itself or being hit by the propellers. The user should be able to launch the drone from their hand, throw it into the air, and catch it at the end of the drone's flight.

Caged drones currently exist, but the ones on the market right now are not designed for the same level of human interaction that the Helosphere is intended for. Skypersonic, Air Hogs, and Interactive Toys have all released a miniature quadcopter, however these drones are designed simply so that the mesh will prevent the propellers from hitting people or walls during flight. The mesh cages for these drones aren't meant to stand up to serious stresses from handling or impact. We wanted to design a cage that could be held in the user's hand, thrown, and caught without serious deformation or breakage.

Most drones on the market are too large to easily handle with one hand. Our design has a six inch diameter, slightly larger than a softball. This ensures that the user can toss and catch it with one hand, making it more of a toy than standard drones. The idea of the Helosphere is to increase interaction with drones, especially among children, to familiarize them with this sort of technology and increase their interest in automated flight and STEM subjects.

Objectives

The main objective of this project is to develop a miniature quadcopter housed inside a mesh cage. The final design should be safe and easy for a human to handle, and strong enough to sustain force from impacts during flight and rough landings. The main objectives revolve around three main areas of the final design, the mesh, chassis, and overall aerodynamics.

The design of the mesh cage surrounding the drone had to be optimized to have a high surface area in order to prevent injury from propellers during handling. However, a higher surface area increases weight and decreases aerodynamic performance, two other factors which need to be optimized. A low surface area also decreases strength, leading to higher deformation and chance of failure during impacts. Therefore, the mesh must be carefully designed to find a middle ground among all of these factors.

The chassis of the drone was extremely important to the overall design, as it must be strong enough to handle the propeller forces and weight of all of the other components without deflecting too much, as high deflection would interfere with the angle of the propellers, causing problems in flight. The chassis must also be lightweight, since the electronic components consist of a high portion of the drone's weight, and if the overall design becomes too heavy, it will not fly properly.

Because this device is designed to fly, aerodynamics are an important factor in the larger components. The mesh must have a low enough surface area that air can pass through it from any direction with minimal turbulence. Aerodynamics are also a

factor in chassis design, since the propellers are attached to the four main arms of the chassis, and air from the propellers must flow past the chassis without impedance.

Modeling

Our first job was to brainstorm mesh designs. After some discussion we decided to pursue two different strategies for creating a mesh. One was to create a hollow sphere and cut holes into it to allow for air flow. This idea created strong shapes, but seemed to leave more to be desired for air flow. These designs were similar to a wiffle ball. The second idea was to create a ball-like structure using rings or struts. This idea would have a lot of air flow but we were worried about the overall strength. Below are four examples of designs we looked at:

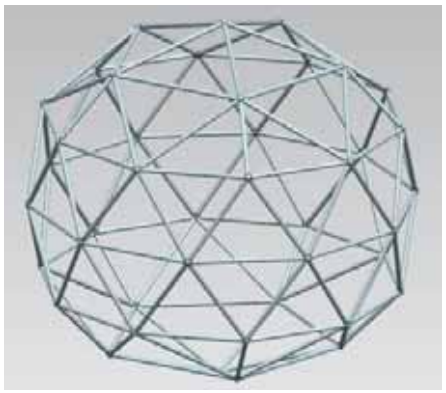

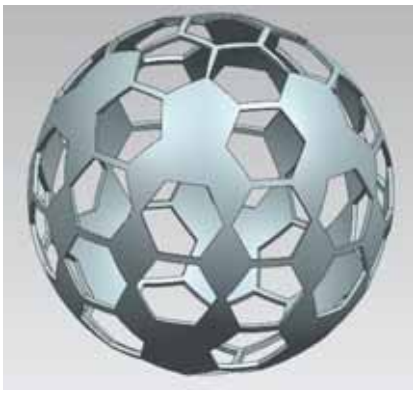

The required priorities for the mesh relate mostly to its strength to weight ratio. This means that it must have a balance of strength under impact and a low overall

weight. In addition to this, it must balance surface area to protect and interact with the user and minimize airflow interruption.

The team started out with three initial designs for the chassis of the drone. These designs are shown below. Each design consists of a complex sketch 150 mm in diameter, extruded 2 mm for the thickness of the frame. Chassis 1 consists of a simple, four arm design, leaving plenty of room for air flow, with 10 mm wide arms to increase strength. Chassis 2 has 5 mm arms for improved aerodynamics around the propellers, with 4 support arms, also 5mm wide, to increase stability. Chassis 3 is essentially the same as chassis 2, but with extra material around the outside edge to minimize deflection while still allowing for air flow from the propellers.

Chassis 1

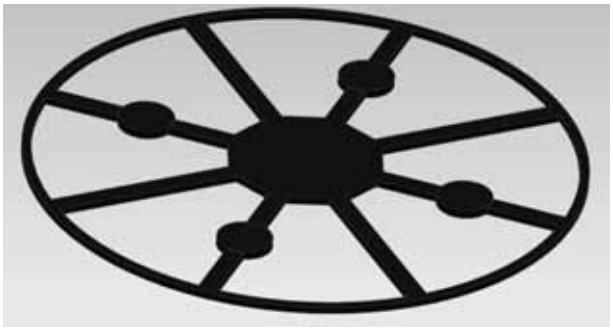

Chassis 2

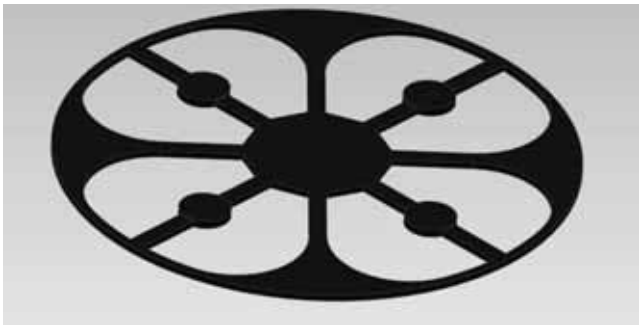

Chassis 3

After a structural analysis was completed on each of the three chassis, chassis 2 was selected as the best design (results discussed in Analysis section). However, it was decided that this design could be optimized further to increase performance. The width of the four supporting arms was decreased from 5 mm to 2.5 mm, and the overall frame thickness was decreased to from 2 mm to 1.5 mm, as this is the standard frame thickness for most miniature quadcopters on the market. Three i.5 mm diameter screw holes were added at each motor mount to secure the motors in place. The final design is shown below.

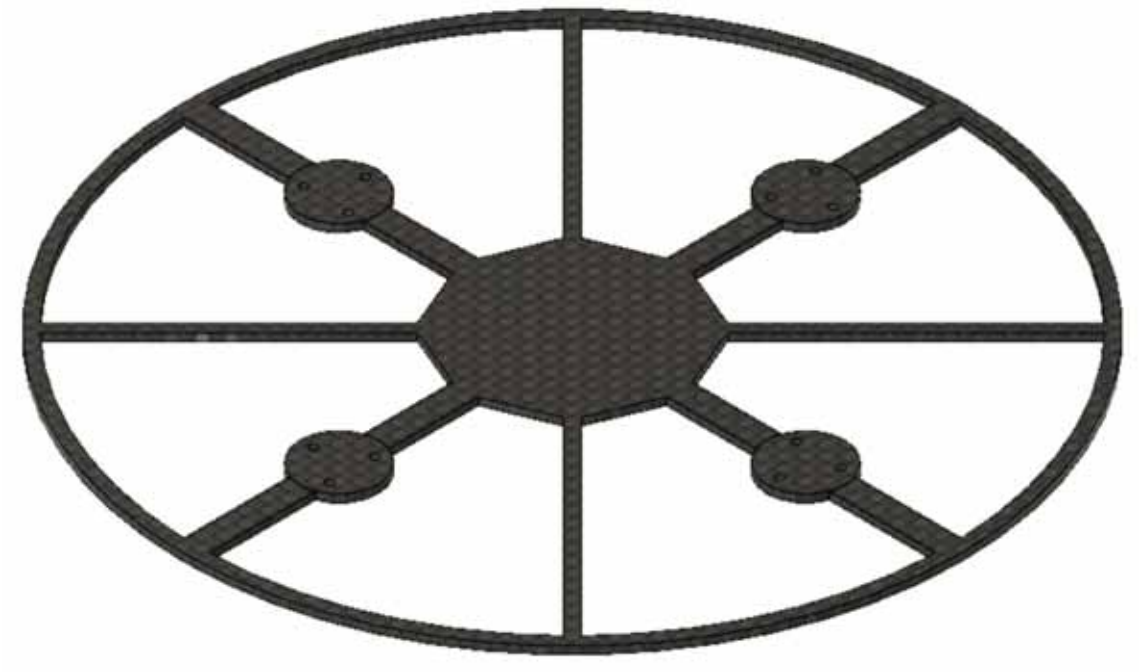

Final Chassis Design

Four 15 mm diameter inboard brushless DC motors were designed to attach to the chassis and control the propellers. The motors were designed by revolving a sketch and then adding an extruded cut at the top for the propellers to fit into, along with three 1.5 mm screw holes on the bottom to secure each motor to the frame. The screws were

designed using extruded circles, an extruded plus-shaped cut out on the top, and the thread function for the actual threads of the screw.

DC Motor

Motor Connection Screw

A rechargeable battery pack and battery mount were designed to be carried underneath the chassis. The mount is designed so that the battery can easily be removed for recharging and quickly inserted for continued use.

Rechargeable Battery and Mount

There were five electrical components associated with the intelligence of the drone. The first is the autopilot/controller of the drone. We modeled this directly after a real item called the “Pixhawk” which is common on many ultralight quadcopters. The decal on top is taken from the chip itself. There is also a chamfer added and extruded cuts where wire ports are.

The autopilot controller comes with a gps and compass board that is hardwired with the controller to increase accuracy and speed of location input which is extremely important for a autonomous quadcopter. The GPS chip is modeled off of that device and is called the “3DR”.

The controller cannot directly send power to the brushless motors for two reasons: it uses 5 volts instead of the required 12 volts, and the control of a brushless motor is too complex. Therefore, to power the motors you also need an electronic speed controller. We also based this model off of an existing component. It takes input from the controller and put the correct amount of energy from another source into each pole of the motor.

The drone will eventually be autonomous but for prototyping and testing it will be necessary to use a radio controller so we added a radio receiver that connects to the controller via USB.

The final electronic component is the camera and distance sensor which gives the autopilot input to move based on as well as a video recording for the person using the device.

The top and bottom views of the assembled drone are below. These assemblies include the main electrical components necessary for the drone's functionality. .

Top View

Bottom View

The view shown below includes the camera/distance sensor combo and propellers added onto the assembly. Two of the propellers rotate clockwise while the other two rotate counterclockwise. This is necessary for quadcopter flight to maintain a stable flight pattern.

Top view of drone assembly including alternating propellers and 4-way cameras and distance sensors.

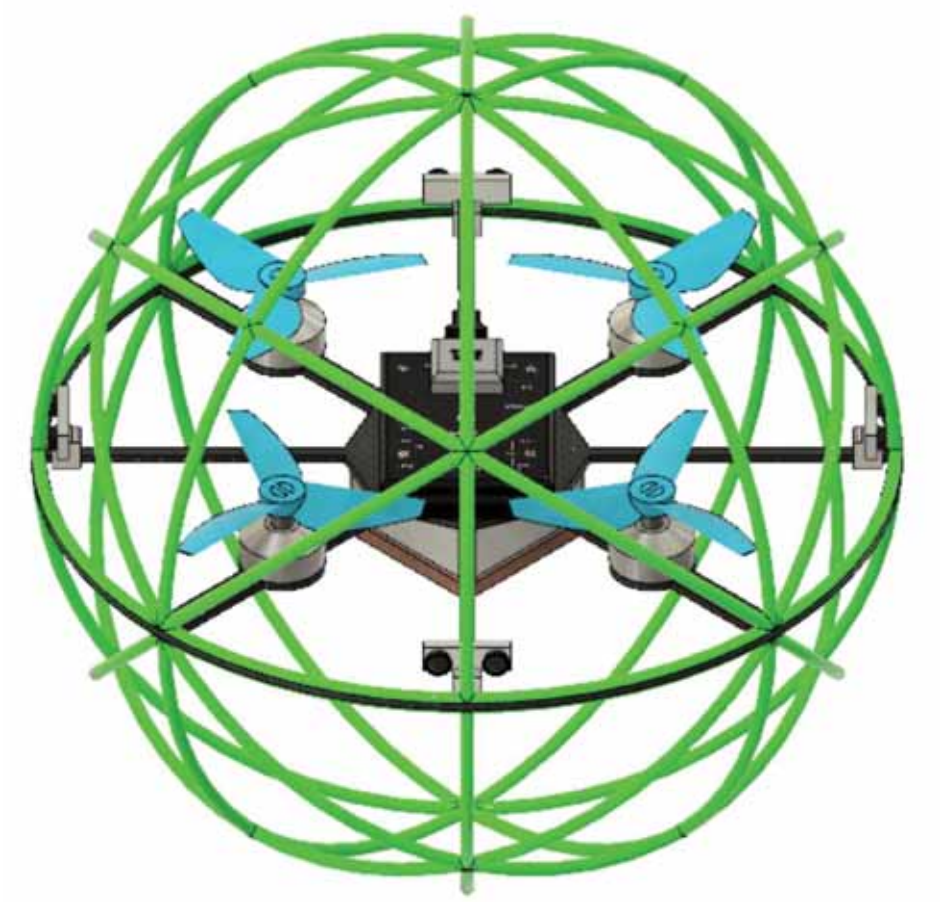

Final Full Assembly

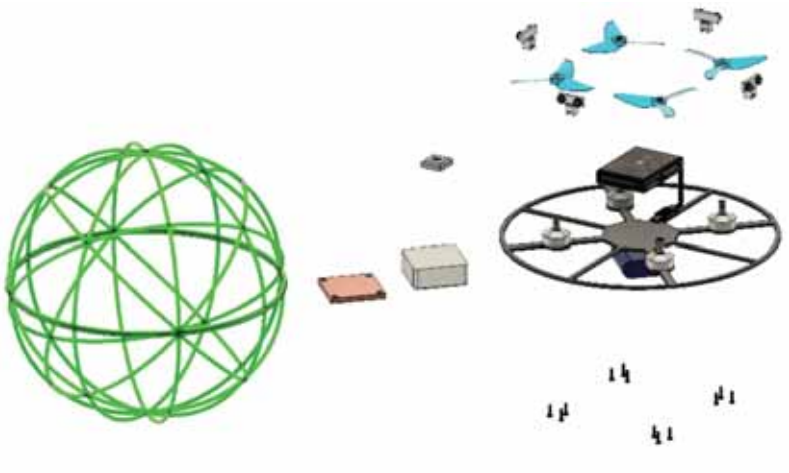

Exploded Full Assembly

Analysis

We had to figure out the best way to analyze and choose between the mesh options. To do this we used 3D modeling software simulations of static stress and structural buckling. To analyze the static stress, we simulated a five pound force on one side of each mesh and locked the other side as if blocked by a hand or wall.

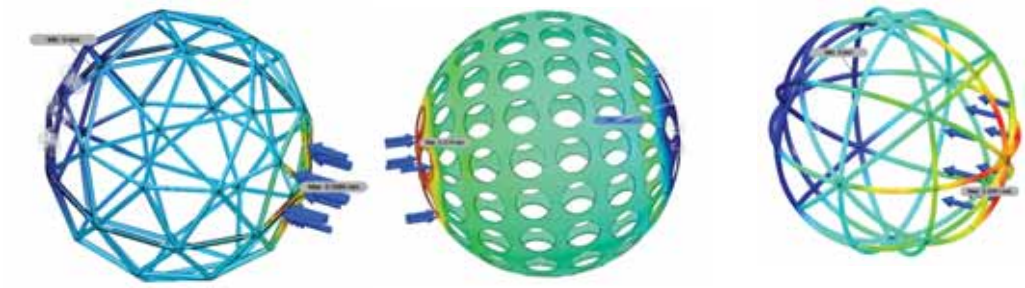

I changed the thickness of each mesh so that the weights would be similar for accurate comparison purposes. Below is a chart of the resultant stress and displacements. As you can see the wiffle ball design is the strongest. However soon we will analyze the air flow to see how these compare in that dimension.

5lbf	**Body 1**	**Body 2**	**Body 3**
Weight (g)	31.182	32.629	34.851

Max Principal Stress (MPa)	4.305	2.35	3.239
Max Displacement (mm)	0.5068	0.217	0.3047

Below is an example of different buckling conditions of each mesh.

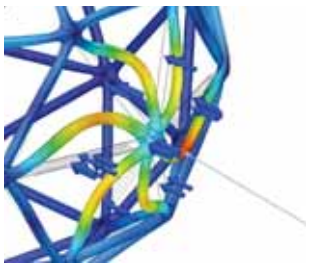
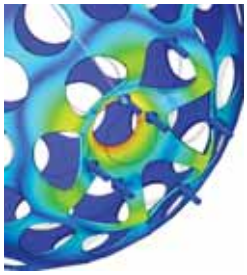


Next we looked at different material choices and how they would affect the strength of the mesh. We used the same five pound force test with different common plastic, below is an analysis of those. Both and PET can be injection molded however ABS is a common 3D print material for testing. We have had several failed attempts at scaled 3D printing. PET is roughly half the cost of ABS by weight. ABS has the best strength to weight and therefore was the best option to move forward with.

Plastics	**PET**	**HDPE**	**ABS**	**PP**
Weight (g)	58.69	36.26	40.37	34.34
Min Safety Factor	14.91	5.629	14.84	8.25
Max Displacement (mm)	0.1685	0.5068	0.1669	0.3461

To finish off the mesh FEA, we wanted to minimize the thickness of the mesh to decrease weight yet maintain strength. Below are photos of each mesh and the strength associated with each on the five pound test. 2.5mm had the most fitting tradeoff of strength to weight.

Thickness (mm)	**2.0**	**2.5**	**3.5**
Weight (g)	13.59	21.01	40.37
Min Safety Factor	2.56	6.271	14.84
Max Displacement (mm)	1.445	0.4977	0.1669

After all of the FEA analysis, the mesh was decided to be the interlocking tori (ring-based) design with a 2.5mm wire diameter and made with ABS. The gap in the center is for the chassis so it can be connected with CA glue.

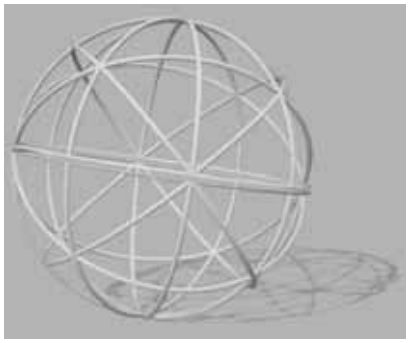

Finite element analysis for the chassis involved a structural analysis simulating a 2:1 thrust ratio. This means that the propellers are outputting a downforce equal to twice the weight of the drone. This is a common scenario in drone flight, especially when the drone is rising directly upwards. For each chassis, there was a fixed restraint around the outside edge of the frame, an upwards force on the motor mounts, simulating the upwards pull of the propellers, an evenly distributed weight force of the frame itself, and a localized weight at the center of the chassis representing the electronic components of the drone. These loads can be seen on chassis 1 below.

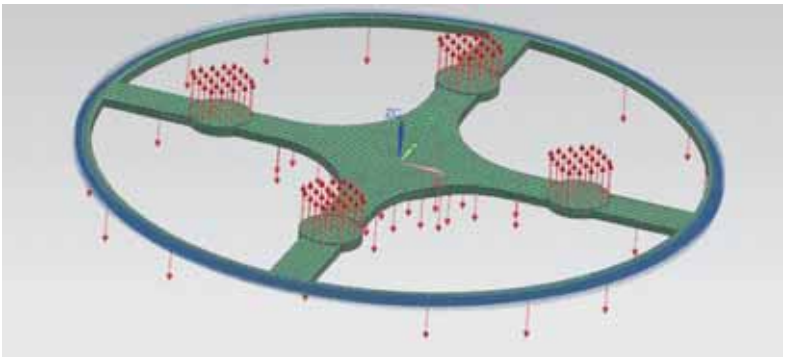

Loads for structural FEA on chassis 1

The results of the three structural analyses are shown in the table below. Chassis 2 was selected out of the three, due to its extremely low maximum principal stress, and comparable weight and maximum displacement to chassis 1.

Chassis Choice	Chassis 1	Chassis 2	Chassis 3
Weight (g)	80.15	84.01	111.20
Max Principal Stress (MPa)	7.836	3.032	4.156
Max Displacement (mm)	0.0312	0.0304	0.0154

Since the max displacement and stress of chassis two were extremely low, we refined it even further by reducing the width of the supporting arms (ones that don't hold motors) from 5 mm to 2.5 mm. Various chassis thicknesses were tested and 1.5 mm was chosen as the optimal thickness due to its low weight but still minimal displacement. This reduction in thickness reduced the frame's weight from approximately 84 grams to 63 grams. Coincidentally, most mini drones with carbon fiber frames use a sheet thickness of 1.5 mm. The structural deformation results for the refined final chassis are shown below.

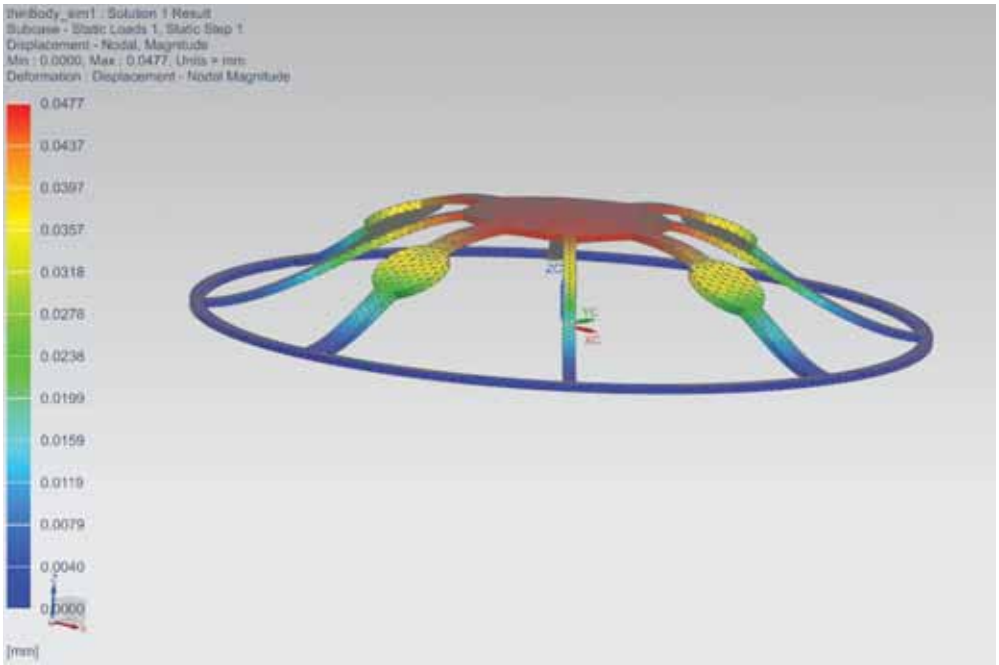

Final Refined Chassis Deformation Results

- Original, 2mm thick, displacement: 0.0152 mm
- 1.5 mm frame, displacement: 0.0477 mm
- 1mm frame, displacement: 0.160 mm
- 0.5 mm frame, displacement: 1.266 mm

Computational Fluid Dynamics were used to analyze the aerodynamics of the mesh ball. The goal was to get an understanding on how the geometry affects the aerodynamics of the device. To get a better idea of how the thrust is going to be deflected because of the balls geometry, a constant 50 mph wind at ambient conditions was applied to the top half of the ball. This is the maximum expected air flow when compared to current drones on the market. CFD was performed on the ‘strongest’ and ‘weakest’ (see FEA above) mesh designs. Streamlines are shown in the analysis to give a better representation of the fluid flow. The weakest, shown on the left, had a very uniform flow indicating little drag. The strongest, shown on the right, had a very nonuniform flow. You can see that the Venturi effect takes place when the fluid is flowing fastest as it escapes through the holes. The escaping air then slows to a slower speed than original indicating more drag. Note the minimum air velocity for the left mesh is 0.22 mi/hr while the right is 0.08 mi/hr minimum, another indication of more drag.

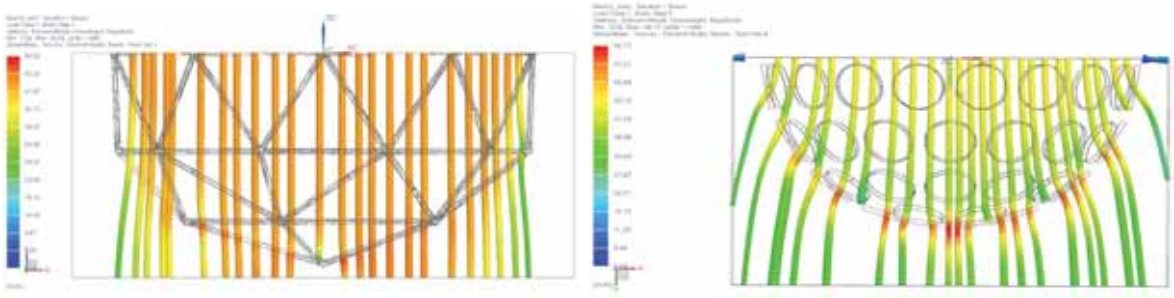

The most optimal design chosen in the FEA was also analyzed with CFD. The results are shown below. The image help visualize how the whole object is interfering with the 50 mi/hr stream of air being applied to the top of the ball. It should be noted that the velocity is slowed when flow is past the mesh. Also note that the minimum velocity of this mesh is 3.45 mi/hr. Indicating less drag than the other two models. This model was both the second best model case for the FEA and the best with CFD. We are most concerned with maximum air flow, therefore we chose to go with this model for our final design.

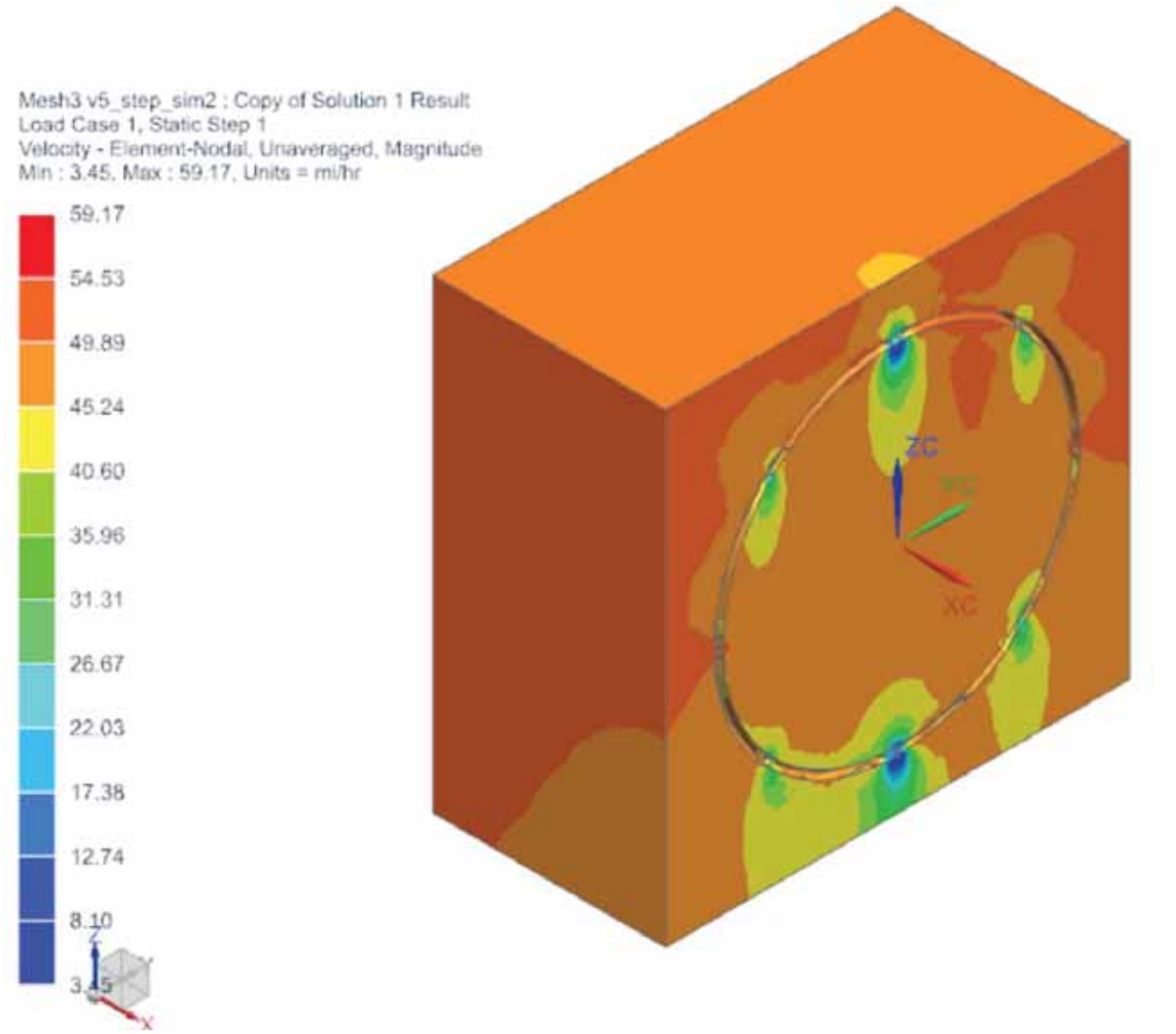

The residual stresses caused by the air flow were also analyzed with 50 mph of wind applied to the top. The results are shown below. These results show that the stresses due to the airflow on the mesh are infinitesimal. The max stress due to the air flow is only 4e-6 Mpa.

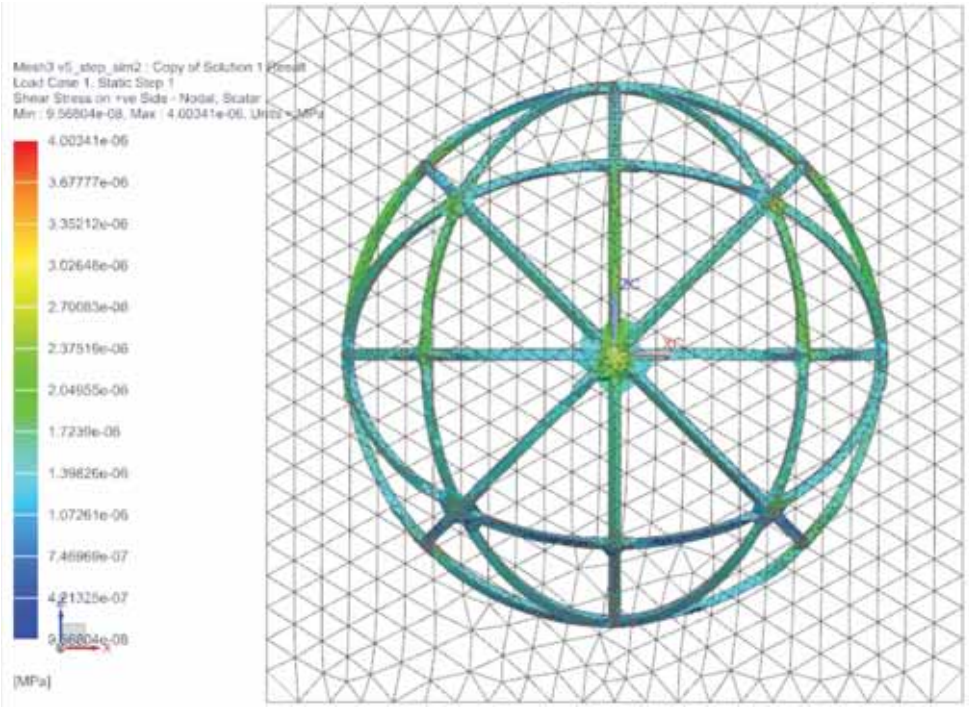

Air flow has an insignificant impact on the stresses of the mesh ball

Verification

Three hand calculations have been completed for the purpose of verifying our FEA and CFD calculations.

In the first calculation, we are simulating throwing the Helosphere into the ground. This is to analyze the strength of the mesh. We simplify the analysis to a ball contacting a solid plane. We are using Polypropylene for the mesh and concrete for the ground. We found the equations for this calculation in Shigley's Mechanical Engineering Design.

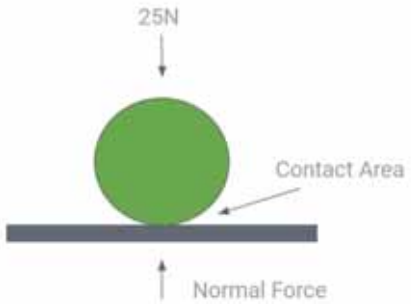

The constants for Polypropylene mesh are:

E_m = 1,300 MPa v_m = 0.35 D = 150mm F = 25N

The constants for the concrete ground are:

E_g = 30,000 MPa v_g = 0.15

The first equation to solve finds the contact area created between the two surfaces:

$$a = \sqrt[3]{\frac{3F}{8}\frac{(1-\nu_1^2)/E_1 + (1-\nu_2^2)/E_2}{1/d_1 + 1/d_2}} \qquad a = \sqrt[3]{\frac{3(25N)}{8}\frac{\frac{(1-(0.35)^2)}{1{,}300MPa} + \frac{(1-(0.15)^2)}{30{,}000MPa}}{\frac{1}{150mm}}}$$

$$\boxed{a = 998.34mm^2}$$

Next we calculate the maximum pressure:

$$p_{max} = \frac{3F}{2\pi a^2} \qquad P_{max} = \frac{3(25N)}{2\pi(998.34\text{mm}^2)^2} \qquad \boxed{P_{max} = 11.93\ MPa}$$

Now we calculate the principal stresses:

z = depth below surface, maximum possible shear stress value at z = 0.5a

$$\sigma_x = \sigma_y \qquad \sigma_x = -P_{max}\left[\left(1 - \left|\frac{z}{a}\right|\tan^{-1}\frac{1}{|z/a|}\right)(1+v) - \frac{1}{2\left(1+\frac{z^2}{a^2}\right)}\right]$$

$$\sigma_x = -11.93MPa\left[\left(1 - \left|\frac{1}{2}\right|\tan^{-1}\frac{1}{|1/2|}\right)(1+0.35) - \frac{1}{2\left(1+\frac{1^2}{2^2}\right)}\right] \qquad \boxed{\sigma_x = 7.76\ MPa}$$

$$\sigma_z = \frac{-11.93MPa}{1+\frac{z^2}{a^2}}$$

$$\sigma_z = \frac{-p_{max}}{1+\frac{z^2}{a^2}} \qquad \boxed{\sigma_z = 9.544MPa}$$

Finally to calculate the maximum shear stress:

$$\tau_{max} = \frac{\sigma_x - \sigma_z}{2} = \frac{\sigma_y - \sigma_z}{2} \qquad \tau_{max} = \frac{-7.76MPa - (-9.544MPa)}{2} \qquad \boxed{\tau_{max} = 1.784MPa}$$

When we compared to these result to the FEA results shown below, we can observe that the maximum principle stress calculated using formulas is almost more than twice the result from the FEA analysis. However this is still in the correct magnitude and the error most likely came from our over-simplification. The FEA uses a complex hollow structure with with several geometries, not just a simple sphere. All of this considered, our percent error of 80% is within our factor of safety for the product and verifies our FEA calculations.

FEA Results

5 lbs-force

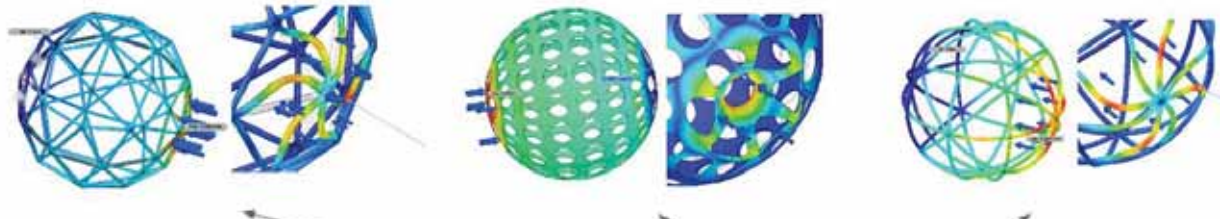

	Body 1	Body 2	Body 3
Weight (g)	31.182	32.629	34.851
Max Principal Stress (MPa)	4.305	2.35	3.239
Max Displacement (mm)	0.5068	0.217	0.3047

The second set of hand calculations are focused on the deflection of the chassis. Specifically, one arm of the frame is treated as a cantilever beam subjected to the weight of the drone's equipment and the thrust from the propellers using a 2:1 thrust ratio, meaning the propellers are outputting a force equal to twice the weight of the drone. This simplified beam model is shown below.

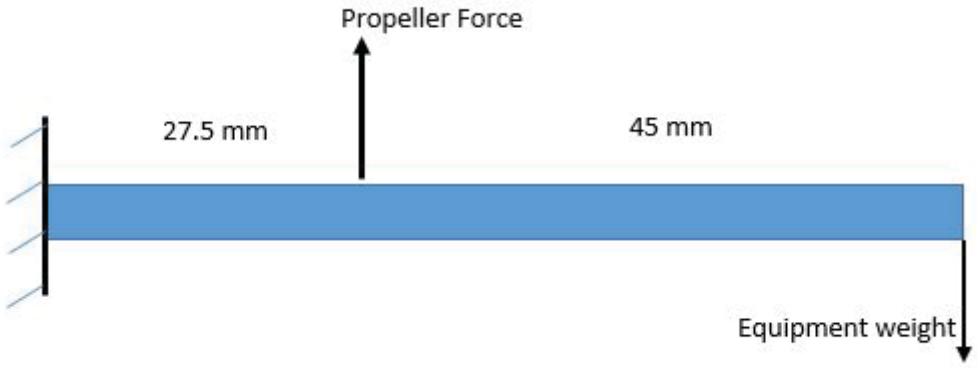

The beam is fixed at the end representing the outer ring of the drone, and the free end represents the center, where the battery and other electronics are secured.

Basic Variables:

L_1=27.5 mm L_1=45 mm E = 70,000 MPa

For a simple rectangular beam, I is calculated as $bh^3/12$. For our arm, this yielded the following result:

$$\frac{(10 \cdot 2^3)}{12} = 6.666$$

But since the arm we are working with has more complex geometry than a simple rectangular beam, the I value calculated from NX, 23.166, was used instead. This value is significantly larger since it accounts for the areas where the beam is wider, specifically the end where it starts to form a platform, and the circle in the middle for the motor mount. The calculations for EI/L^3 for the first and second sections of the beam are shown below.

$$Section1: \frac{EI}{L^3} = \frac{70000(23.166)}{27.5^3} = 77.97 \quad Section2: \frac{EI}{L^3} = \frac{70000(23.166)}{45} = 17.80$$

The matrix calculations began with section 1:

$$\begin{bmatrix} F_1 \\ m_1 \\ F_2 \\ m_2 \\ F_3 \\ m_3 \end{bmatrix} = \frac{EI}{L_1^3} \begin{bmatrix} 12 & 6L_1 & -12 & 6L_1 & 0 & 0 \\ 6L_1 & 4L_1^2 & -6L_1 & 2L_1^2 & 0 & 0 \\ -12 & -6L_1 & 12 & -6L_1 & 0 & 0 \\ 6L_1 & 2L_1^2 & -6L_1 & 4L_1^2 & 0 & 0 \\ 0 & 0 & 0 & 0 & 0 & 0 \\ 0 & 0 & 0 & 0 & 0 & 0 \end{bmatrix} \begin{bmatrix} d_1 \\ f_1 \\ d_2 \\ f_2 \\ d_3 \\ f_3 \end{bmatrix}$$

Most of the matrix work was done in excel in order to save time. Process shown below.

		Matrix 1							Matrix 1 * EI/L1^3			
12	165	-12	165	0	0		935.6906	12865.75	-935.691	12865.75	0	0
165	3025	-165	1512.5	0	0		12865.75	235872	-12865.7	117936	0	0
-12	-165	12	-165	0	0		-935.691	-12865.7	935.6906	-12865.7	0	0
165	1512.5	-165	3025	0	0		12865.75	117936	-12865.7	235872	0	0
0	0	0	0	0	0		0	0	0	0	0	0
0	0	0	0	0	0		0	0	0	0	0	0
		Matrix 2							Matrix 2 * EI/L2^3			
0	0	0	0	0	0		0	0	0	0	0	0
0	0	0	0	0	0		0	0	0	0	0	0
0	0	12	106.7733	-12	106.7733		0	0	213.5467	1900.091	-213.547	1900.091
0	0	106.7733	1266.727	-106.773	633.3636		0	0	1900.091	22542.11	-1900.09	11271.06
0	0	-12	-106.773	12	-106.773		0	0	-213.547	-1900.09	213.5467	-1900.09
0	0	106.7733	633.3636	-106.773	1266.727		0	0	1900.091	11271.06	-1900.09	22542.11

Once the matrices on the left were formed, they were multiplied by their respective EI/L^3 values in order to find the matrices on the right. MAtrix 1 corresponds to the left half of the simply supported beam, and matrix 2 corresponds to the right half, or the free end. Finally, these matrices were added together to get the final matrix for the system of equations.

		Combined Matrix			
935.6906	12865.75	-935.691	12865.75	0	0
12865.75	235872	-12865.7	117936	0	0
-935.691	-12865.7	1149.237	-10965.7	-213.547	1900.091
12865.75	117936	-10965.7	258414.1	-1900.09	11271.06
0	0	-213.547	-1900.09	213.5467	-1900.09
0	0	1900.091	11271.06	-1900.09	22542.11

Once this matrix was plugged into the full system, d_2 and d_3 could be solved for. The results were: d_2=0.015 mm and d_3=0.005 mm. The FEA results are shown below.

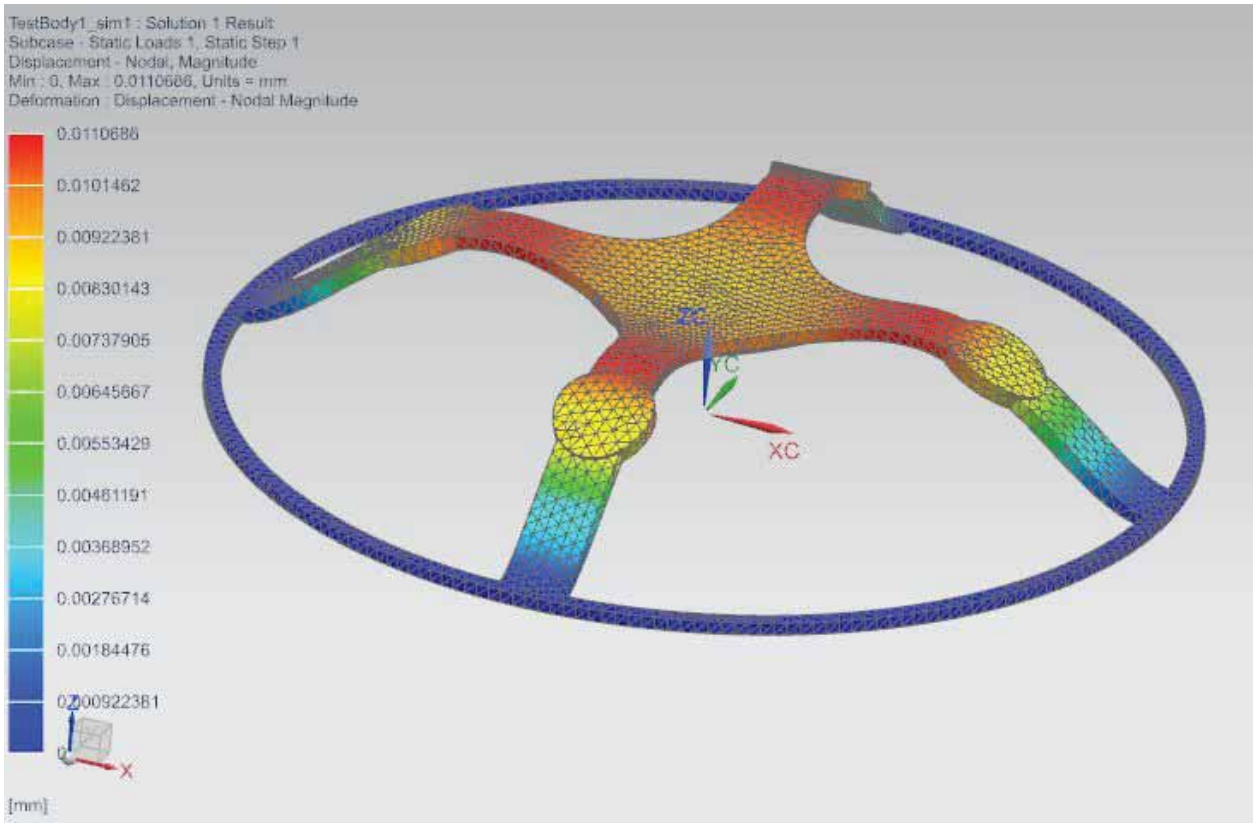

In this picture, the maximum displacement is ~0.0111 mm. This occurs not at the motor's centerpoint, but just after it. The displacement at the center of the drone, where the end of the simple beam model would be, is approximately 0.0085 mm.

Percent error:

$$d_2\ Percent\ error = \frac{calculated - actual}{acctual} = \frac{0.015 - 0.0111}{0.0111} = 35\,\%$$

$$d_3\ Percent\ error = \frac{calculated - actual}{acctual} = \frac{0.005 - 0.0085}{0.0085} = 41\,\%$$

Possible explanations:

The calculated deflection of the motor position was higher than the maximum deflection in the NX model. This could be due to the fact that the thrust was treated as a

vector force, instead of affecting an entire area of the beam. This could have caused the theoretical beam to deflect more sharply than the NX model. The extra circle of material in the real world arm may also provide strength to that area, causing less deflection in that particular spot, and more deflection immediately after the motor mounts.

The calculated deflection at the end of the beam was less than the NX model. This is likely due to the fact that in the calculations, the weight of the equipment was all placed at the end of the beam, rather than spread out over an area. This caused a sharper downward deflection, cancelling out more of the upwards deflection in the hand calculations than in the NX model.

The hand calculations for the CFD calculations are quite difficult to model accurately. Some assumptions can be made to give a reasonable estimate of the drag and speeds we may see by using Bernoulli's equation and the drag equation. Assuming the ball is a solid sphere and the wind is 50 miles an hour. Assuming standard atmospheric conditions, the reynolds number is 2.30x10^5. At this reynolds number, the coefficient of drag across a rough sphere is approximately 0.3. [1] Therefore:

$$D = Cd * 0.5 * rho * V^2 * A$$

$$D = 0.3 * 0.5 * 1.225 kg/m^3 * 0.225 m^2$$

$$D = 0.4\ Newtons$$

The drag found in NX on the chosen mesh ball was 0.61 Newtons. This results in a surprisingly low 52% error. This error is due to the fact that a solid ball was compared to a mesh ball. The solid ball had less drag because the flow around the ball was less turbulent, causing less drag.

With the mesh ball, the flow becomes turbulent around the wires, causing more drag. There is no good way to model this system by hand because it is such a complex shape.

Summary and Future Work

Designing the Helosphere required several types of analysis in order to balance three main requirements: strength, weight, and air flow. For the mesh, we needed to choose between various shapes and materials. Then we minimized the thickness relative to those choices. For the chassis, we knew we would use carbon fiber for its strength, inflexibility, and common use in the industry. We analyzed shape and used the resulting strength to minimize the shape and thickness and therefore weight.

We used CFD to calculate air speed and visualize streamlines around and through the mesh. This helped us decide which shapes we should eliminate from our design options.

We verified the FEA and CFD analysis we did with hand calculations. The were associated with stress, deflection, and drag force.

We finally used the information we had learned from our analysis to model the prototype. We included the electronics to run the device without the wires connecting them because we don’t know how the will be mounted yet. The model turned out great and are excited to see how it will look assembled in real life.

Future improvements for this product will be centered around increasing mobility and smooth transitions between throwing the drone and stable flight. This could involve implementing a gyroscope system so that no matter how the drone is gripped or thrown,

the propellers can always face up so that the drone is ready to fly in the correct direction. The implementation of a gyroscope could also allow the drone to roll along the ground using its propellers as propulsion.

Another possible improvement would be the addition of inductive charging on the bottom of the mesh so that the drone could land on a charging pad when its battery is low, recharging itself until it is ready for flight.

In order to mass produce this product, it would also be necessary to design specifically for manufacture by optimizing the parts to whatever process is used to create them (i.e. 3D printing vs injection molding for the mesh).

Lastly, software would need to be developed to make this drone relatively autonomous and programmable, allowing the user to give commands, such as follow the controller, return when thrown, etc.

Sources:

[1]

Grc.nasa.gov. (2019). *Drag of a Sphere*. [online] Available at:

https://www.grc.nasa.gov/www/k-12/airplane/dragsphere.html [Accessed 26 Apr. 2019].